Pharmaceutical Research, Vol. 22, No. 8, August 2005 (© 2005)
DOI: 10.1007/s11095-005-5264-x

Research Paper

Bridging the Pharmacokinetics and Pharmacodynamics of UK-279,276 Across Healthy Volunteers and Stroke Patients Using a Mechanistically Based Model for Target-Mediated Disposition

E. Niclas Jonsson,[1,4] Fiona Macintyre,[2] Ian James,[2] Michael Krams,[3] and Scott Marshall[2]

Received November 5, 2004; accepted March 15, 2005

Purpose. UK-279,276 is a recombinant glycoprotein and is a selective antagonist of CD11b, which in preclinical models of acute stroke blocks the infiltration of activated neutrophils into the site of infarction. Binding of UK-279,276 to the CD11b receptors is hypothesized to facilitate its elimination. The event of an acute stroke leads to proliferation of neutrophils and an up-regulation of CD11b, which results in different pharmacokinetics/pharmacodynamics (PK/PD) in patients than in healthy volunteers. The aim of this current analysis was to develop a mechanistically based model to bridge the differences between healthy volunteers and patients.

Methods. PK samples, neutrophil counts, and total number and number of free CD11b receptors per neutrophils from three healthy volunteer studies (n = 98) and one patient study (n = 169) were modeled using the mixed effects modeling software NONMEM version VI (beta). Three mechanistic submodels were developed based on underlying physiology and pharmacology: (1) neutrophil maturation and proliferation, (2) CD11b up-regulation, and (3) three clearance pathways for UK-279-276 including CD11b-mediated elimination.

Results. The model accurately described the time course of CD11b expression, CD11b binding, and the measured PK of UK-279,276 and accounted for the PK/PD differences between healthy volunteers and patients.

Conclusions. A complex mechanistic model that closely resembled the "true" underlying system provided an effective bridge between healthy volunteers and patients by appropriately accounting for the underlying disease-dependent target mediated disposition.

KEY WORDS: CD11b; mechanistic models; NONMEM; pharmacodynamics; pharmacokinetics; stroke.

INTRODUCTION

The effective integration of discrete studies and the ability to predict from one population to another is key to the successful application of accumulated drug development knowledge. The development of a holistic pharmacokinetic/pharmacodynamic (PK/PD) model often provides an important bridge between studies and study populations. Recombinant neutrophil inhibitory factor (UK-279,276) was under development as a potential treatment for acute ischemic stroke. In the development program, both healthy volunteers and patients were studied to assess the effect of UK-279,276 on acute ischemic stroke.

UK-279,276 is a recombinant glycoprotein of 48 kDa originating from canine hookworm and is a selective antagonist of CD11b (the α-subunit of the adhesion integrin, CD11b/CD18, also known as Mac-1). The binding of UK-279,276 to CD11b/CD18 blocks a number of neutrophil adhesion-dependent functions mediated by Mac-1, for example, the infiltration of activated neutrophils to the site of infarction (1,2). The hypothesis rests on the fact that neutrophil infiltration and the release of neuroactive factors play a role in the final phases of neuronal injury following stroke and that the interaction between neutrophils and endothelium is the critical factor that determines neutrophil transmigration to the site of the infarct (3–5). Although UK-279,276 was not shown to be effective in the treatment of the general ischaemic stroke population (6), it may have a potential role as a therapeutic agent in the treatment of reperfusion injury (7).

Binding of UK-279,276 to the target (CD11b) is hypothesized to also facilitate its clearance through internalization and subsequent degradation of the drug-receptor complex. The complexity of the interaction is increased further by temporal changes in the number of circulating neutrophils and therefore binding sites that occur as a consequence of an acute stroke (an initial increase in the levels are followed by a gradual decline back to normal levels). In contrast, the

[1] Division of Pharmacokinetics & Drug Therapy, Department of Pharmaceutical Biosciences, Uppsala University, Box 591, SE-751 24 Uppsala, Sweden.
[2] Department of Clinical Pharmacology, Pfizer Global Research & Development, Sandwich, UK.
[3] Department of Experimental Medicine, Pfizer Global Research & Development, Groton, Connecticut 06340, USA.
[4] To whom correspondence should be addressed. (e-mail: Niclas.Jonsson@farmbio.uu.se)

ABBREVIATIONS: PD, pharmacodynamics; PK, pharmacokinetics.

neutrophil levels are generally constant over time in healthy volunteers. The effect of stroke on the circulating neutrophils may therefore lead to differences in the time course of the PK/PD between patients and healthy volunteers.

The PK/PD data described in this article were initially analyzed using a series of empirical models: two- and three-compartment models with receptor binding and combinations of linear and nonlinear elimination processes. Although separate models could describe the two populations individually, it was not possible to find a single model that could describe all the data and therefore bridge between healthy volunteers and patients. The apparent difference between healthy volunteers and patients was considered to be an artifact of the empirical nature of the models tested. A PK/PD/disease model that more closely reflects the "true" underlying biology through the incorporation of an understanding of neutrophil dynamics after stroke would avoid such artifacts and hence better describe the data from both healthy volunteers and patients. The aim of this article was therefore to develop a mechanistically based model for the neutrophil dynamics after stroke and the receptor binding and PK disposition, to bridge the PK/PD differences between healthy volunteers and patients treated with UK-276,279.

MATERIAL AND METHODS

Data Used in the Analysis

The data used in the analysis come from four studies—three healthy volunteer studies (studies 1, 2, and 4) and a patient safety and tolerability study [study 3 (8)]. Detailed descriptions of the studies, including study type, study subject type, dose sizes, and sampling times, are displayed in Table I. The studies were performed in accordance with the declaration of Helsinki and approved by the relevant regulatory and ethics committees.

Patients and healthy volunteers were administered one dose of UK-279,276 as a 15-min IV infusion. PK samples and neutrophil counts were taken in all studies and total number and free number of CD11b receptors per neutrophil were measured in studies 2–4.

The PK samples were analyzed by using a dissociation-enhanced lanthanide fluorescence immunoassay to detect unbound UK-279,276.

The CD11b/CD18 occupancy assay was developed using flow cytometry as an analytical platform. In brief, anticoagulated blood samples were incubated with a cocktail of two anti CD11b antibodies conjugated to different fluorescent labels. One antibody binds to CD11b irrespective of whether UK-279,276 is bound, thus measuring total amount of CD11b present on the surface of the neutrophil. A second antibody binds to CD11b competitively with UK-279,276, thus determining the amount of unoccupied CD11b receptors. The exact antibody-to-fluorophore ratio was determined for each antibody and the flow cytometer calibrated using fluorescently labeled beads relevant to each of the fluorophores utilized, enabling the antibody binding capacity and subsequently the percentage occupancy to be calculated for each sample. Samples were processed at the clinical sites and the antibody staining (binding) procedure performed on ice to prevent *ex vivo* up-regulation of CD11b. Samples were then fixed with paraformaldehyde and shipped to the assay laboratory for flow cytometry analysis. Initially the incubation temperature was 37°C (study 2) and for later studies it was reduced to 4°C, resulting in decreased *ex vivo* up-regulation of CD11b expression and reduced variability.

The covariates sex, age (both categorical young/elderly and continuous), body weight, and dose were available from all four studies.

MODELING

All the modeling was performed using NONMEM version VI (beta) software (9) employing nonlinear mixed effects models and the first-order estimation method (the more sophisticated first-order conditional estimation method could not be used owing to numerical difficulties). Graphical goodness of fit assessment was facilitated by the use of Xpose (10). Statistical model discrimination was based on the objective function value (OFV) provided by NONMEM. The difference in the OFV from two hierarchical models is approximately χ^2-distributed and can therefore be used to assign significance levels for model improvements. However, because it was necessary to use the first-order method in this analysis, the nominal significance levels obtained based on the OFV differences can be anticipated to be different from the nominal ones (11,12). Therefore it was decided to use an OFV difference of 10 to assign statistical significance.

Candidate covariate relationships were identified on mechanistic grounds and included in the model if they showed statistical significance.

Model Development

Prior to building a model for the binding to and potential elimination of UK-279,276 via the CD11b/CD18 receptors in patients, it was necessary to account for the dynamic changes in the total receptor expression after a stroke. This means that since the number of receptors was measured per neutrophil, it was necessary to account for the changing levels of neutrophils. A further complication was that CD11b/CD18 is also present on other blood cell types, for example, monocytes (13). Thus non-neutrophilic CD11b/CD18 may also be involved in UK-279,276 elimination. Finally, data from the rat and the dog indicated that UK-279,276 may also be metabolized via desialylation in the liver (14).

The strategy for the model development was therefore to build three submodels: one model for the neutrophils, one for the receptors, and one for the PK. The neutrophil model drives the receptor expression, which in turn influences the PK of UK-279,276.

When inter-individual variability was modeled, individual parameter estimates were assumed to vary exponentially around the corresponding typical parameter value for the population:

$$P_i = P \cdot e^{\eta_{P,i}} \quad (1)$$

where P is the typical value of the parameter in the population, P_i is the ith individual's value of parameter P, and $\eta_{p,i}$ is a symmetrically distributed variable with standard deviation ω_P. Hereafter, a subscript i on a parameter is used

Table I. Description of the Studies Used

Study	Study description	Number of individuals	Number of PK observations	Number of neutrophil observations	Number of free CD11b observations	Number of total CD11b observations	WT [Kg: median (range)]	SEX (M/F)	AGE years: median (range)]	Doses
1	Safety and toleration study in healthy male volunteers	51	472	720	–	–	73 (60–96)	51/0	24 (18–42)	0.006, 0.02, 0.06, 0.2, 0.5 and 1 mg/Kg
2	Safety and toleration study in healthy male and female volunteers	32	473	451	244	184	71 (60–91)	29/3	30 (19–70)	0, 0.2, 1.25 and 1.5 mg/Kg
3	Safety and toleration study in male and female stroke patients (6)	169	1646	623	991	757	73 (38–113)	102/67	73 (39–92)	0, 0.06, 0.1, 0.2, 0.5, 1 and 1.5 mg/Kg
4	Safety and toleration study in healthy elderly volunteers	15	143	149	207	155	71 (54–100)	8/7	68 (65–74)	0, 0.06, 0.1, 0.5 and 1 mg/Kg
	Total:	267	2734	1943	1442	1096	74 (±13)[a]	190/77	60 (±30)[a]	

[a]Mean ± sd.

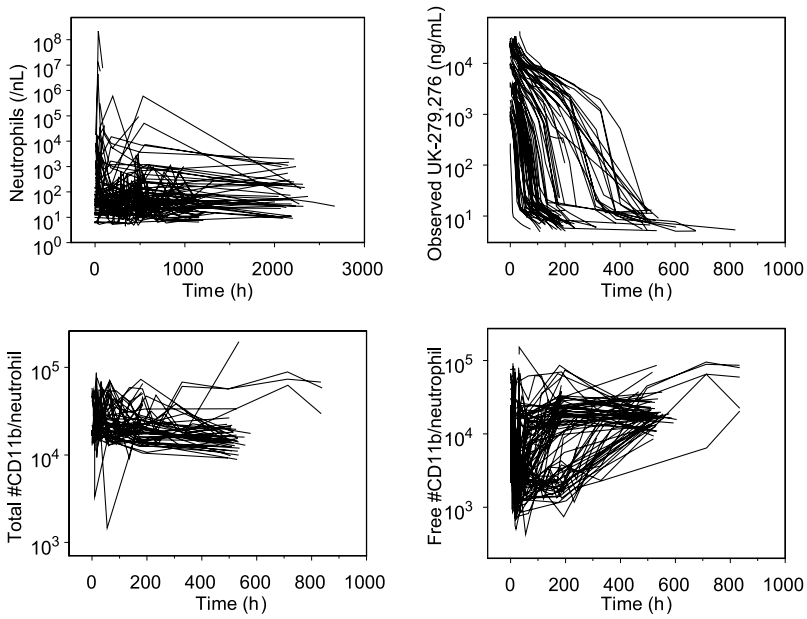

Fig. 1. The observed data used in the analysis. The top left panel shows the observed neutrophil counts *vs*. time, the top right panel shows the observed UK-279,276 concentrations *vs*. time, the bottom left panel shows the total number of CD11b receptors per neutrophil *vs*. time, and the bottom right panel shows the number of free CD11b receptors per neutrophil. Each individual's observations are connected with a line. The graph displays a random selection (same selection in all panels) of about 40% of the total number of individuals.

to indicate that inter-individual variability was modeled for that parameter. The number of inter-individual variability terms was determined based on the data.

Additive, proportional, and slope intercept models for both the log-transformed and nontransformed data were considered in estimating the residual variability.

RESULTS

A total of 267 individuals from all four studies were available for analysis. The number of observations was 2734, 1943, 1442, and 1096 for PK, neutrophils, number of free CD11b/CD18 receptors per neutrophil, and total number of CD11b/CD18 receptors per neutrophil, respectively. The observed data are depicted in Fig. 1 and summarized by study in Table I.

THE NEUTROPHIL MODEL

The model for the neutrophils (Fig. 2) was inspired by the general model for white-blood cell proliferation and maturation suggested by Friberg *et al*. (15) but reformulated

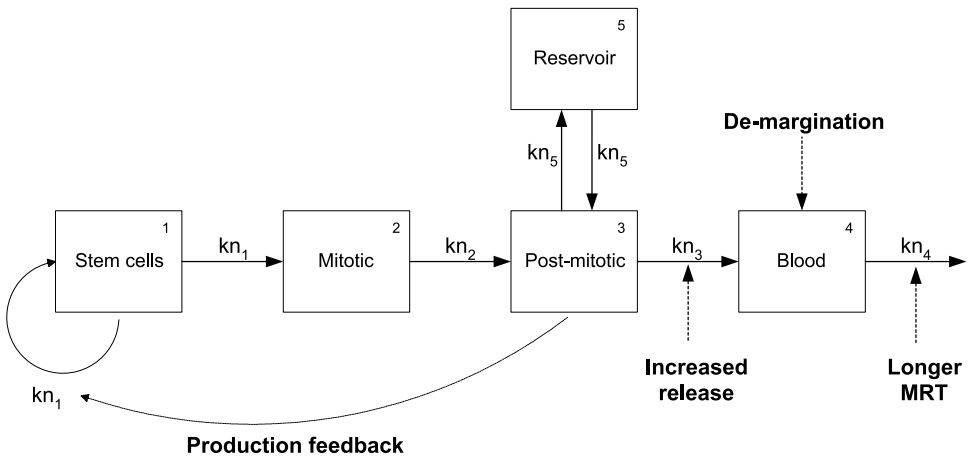

Fig. 2. The neutrophil model. Compartments are numbered 1–5 in the order stem cells, mitotic, post-mitotic, blood, and reservoir. Dashed arrows indicate processes that are patient specific.

according to Walker and Willemze (16). It consists of a stem cell compartment with auto-generation of new stem cells. This compartment is linked to a mitotic compartment, which in turn is linked to a post-mitotic compartment. Neutrophils are released from the latter compartment into a blood compartment. A reservoir compartment is linked to the post-mitotic compartment. Since not all parameters of this model are identifiable, some of the parameters were fixed to the literature values. Thus, the mean transit times through the mitotic and post-mitotic compartments were fixed to 120 and 168 h, respectively (16), the initial ratio between the levels in the post-mitotic and the reservoir were also set to unity, and the mean residence time of the neutrophils in blood for healthy volunteers was set to 7 h (16).

The neutrophil model for healthy volunteers was mathematically described by this system of differential equations:

$$\begin{aligned}
\frac{dA1}{dT} &= kn_{1,i} \cdot (A1 - A1) \\
\frac{dA2}{dT} &= kn_1 \cdot A1 - kn_2 \cdot A2 \\
\frac{dA3}{dT} &= kn_2 \cdot A2 - (kn_3 + kn_5) \cdot A3 + kn_5 \cdot A5 \\
\frac{dA4}{dT} &= kn_3 \cdot A3 - kn_4 A4 \\
\frac{dA5}{dT} &= kn_5 \cdot (A3 - A5)
\end{aligned} \tag{2}$$

where kn_{1-5} are the rate constants for mass transfer between the compartments and A1–A5 are the amounts of mass in the compartments (according to the compartment numbering in Fig. 2). The model fitted to the data was parameterized in terms of residence times (i.e., the inverses of kn_2, kn_3, and kn_4) MRT_2, MRT_3, and MRT_4 except for kn_1, which were estimated directly and kn_5, which were fixed to unity.

At time zero (just before a stroke in the case of patients) the neutrophil system was assumed to be at steady state and the initial conditions for (2) were therefore set to be A1(0) = 1, A2(0) = kn_1/kn_2, A3(0) = kn_1/kn_3, A4(0) = $Base_{HV}$ and A5(0) = A3(0), in which $Base_{HV}$ is a parameter to be estimated and represents the baseline level of the neutrophil counts in healthy volunteers.

Four processes were used to account for the dynamic changes in the neutrophil counts after stroke. The first process was an instantaneous increase in the neutrophil levels in plasma. This can be viewed as a change in the ratio of de-marginated to marginated neutrophils (16). This was accomplished by letting the patients have a different A4(0).

$$Base_P = Base_{HV} \cdot (1 + MARG) \tag{3}$$

where MARG is the fractional change in the initial neutrophil levels for patients compared to healthy volunteers.

The second process was an increased release from the post-mitotic compartment to blood. This also leads to a shift in the ratio of precursor neutrophils from the reservoir to the post-mitotic compartment. This increased release was assumed to decrease with time in an exponential fashion (that could be characterized by a half-life). Therefore, the equation for the mass-transfer rate constant for patients between the post-mitotic and blood compartment ($k_{3,P}$) was described by:

$$kn_{3,P} = \frac{1}{MRT_3 - K_{max} \cdot e^{-\ln 2 \cdot T / t_{K_{max}}}} \tag{4}$$

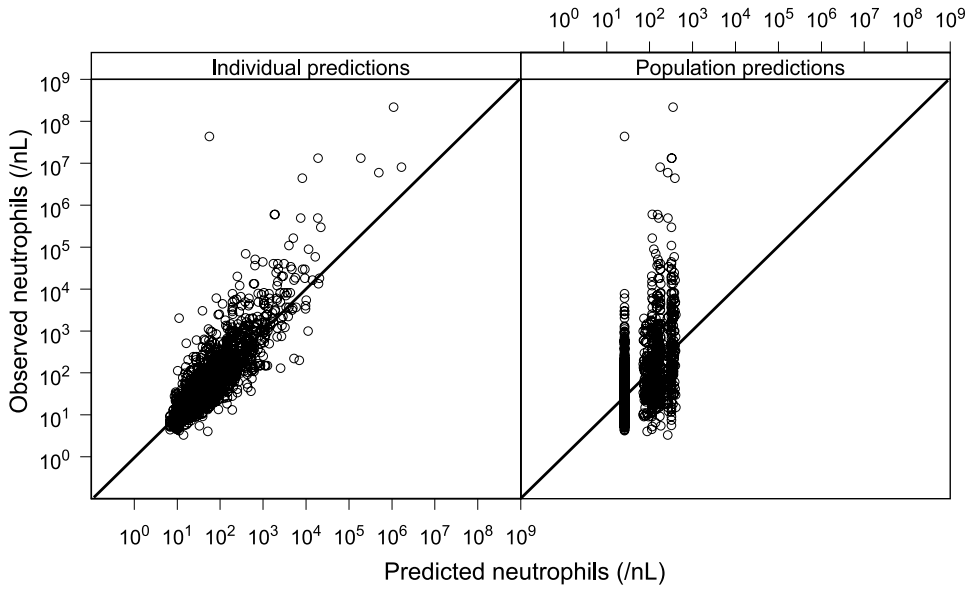

Fig. 3. Goodness of fit plots for the neutrophil model. Shown in the left and right panels are the observed neutrophil levels *vs.* the corresponding predictions based on the individual and population parameter, respectively. The diagonal lines are the lines of identity.

Table II. Parameter Estimates for the Neutrophil Model

		Estimate	RSE (%)
kn_1	(1/h)	0.466	2.0
K_{max}	(h)	48.9	0.48
t_{Kmax}	(h)	52.0	0.23
MSTEP	(%)	0.461	9.1
δ		0.0357	2.7
MARG	(%)	0.771	5.8
ω_{kn1}	(%)	13	13[a]
ω_{MSTEP}	(%)	54	37[a]
σ_{NC}	(%)	21	7[a]

[a] The RSE is given for the variance of the parameter and not the standard deviation.

K_{max} is the maximum decrease in the post-mitotic residence time and t_{Kmax} is the half-life for the return to the pre-stroke residence time. K_{max} for healthy volunteers was set to zero.

The third process was an increased residence time of neutrophil in plasma (16). Clearly, this increase would return to the baseline residence time with time. This return to baseline occurred very slowly, however, and could not be characterized, that is, patients were allowed to have a longer half-life throughout the observed time period. The patient rate constant for neutrophil elimination from the blood compartment ($kn_{4,p}$) was modeled as:

$$kn_{4,p,i} = \frac{1}{MRT_4(1 + MSTEP_i)} \tag{5}$$

The fourth process was a feedback from the post-mitotic state to the auto-generation rate of stem cells (15). The feedback signal was implemented by changing the differential equation for the stem cell compartment in Eq. (2) according to Eq. (6).

$$\frac{dA1}{dT} = kn_{1,i} \cdot \left(A1 \cdot \left(\frac{A3(0)}{A3} \right)^{\delta} - A1 \right) \tag{6}$$

δ is a parameter that governs the size of the feedback signal. These four processes that were used to account for the post-stroke changes in neutrophil dynamics were all estimated and supported by the data. The fit of this model to the neutrophil counts was quite adequate, as shown in Fig. 3 and the parameter estimates are tabulated in Table II.

THE MODEL FOR THE TOTAL NUMBER CD11b RECEPTORS PER NEUTROPHIL

The total number of CD11b receptors per neutrophil in healthy volunteers showed no distinctive patterns and was set to be constant. In patients, on the other hand, the counts appeared to be higher at early time points with a gradual decline over time. This was modeled according to the following differential equation:

$$\frac{dA6}{dT} = Rate_{CD} \cdot \left(1 + CD_{max} \cdot e^{-\ln 2 \cdot T / t_{CD\,max,i}} + \theta_{study2}\right) - A6 \cdot 1/MRT_{CD,i} \tag{7}$$

A6 is the total number of CD11b receptors per neutrophil. $Rate_{CD}$ is the turnover rate of CD11b receptors on neutrophils in healthy volunteers. CD_{max} is a parameter that quan-

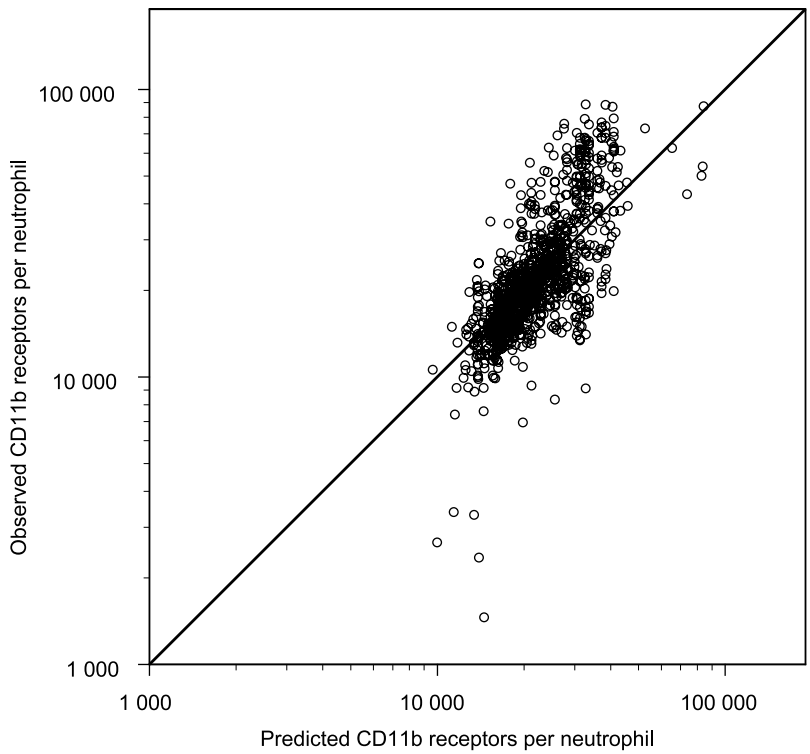

Fig. 4. Goodness of fit plots for the model describing the number of CD11b receptors per neutrophil. The observed number of CD11b receptor per neutrophil are plotted *vs.* the individual predictions. The diagonal line is the line of identity.

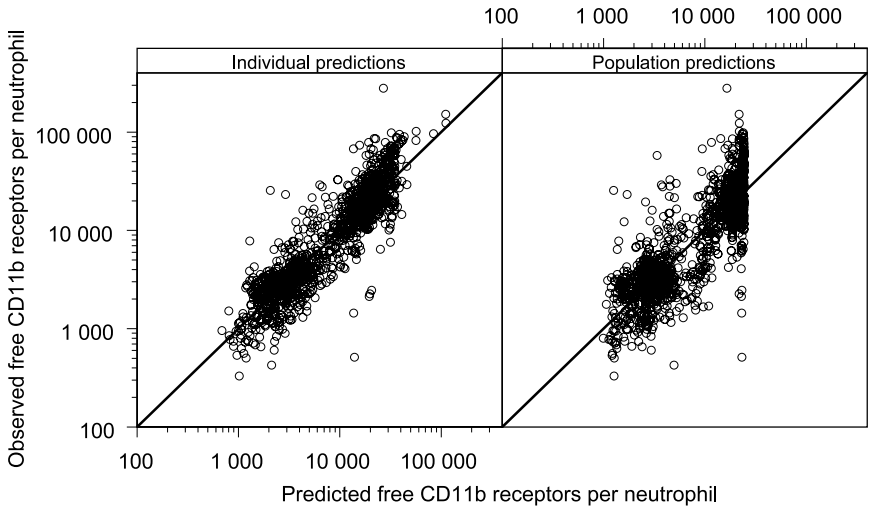

Fig. 5. Goodness of fit plots for the free CD11b receptor model. Shown in the left and right panels are the observed free CD11b receptor levels *vs.* the corresponding predictions based on the individual and population parameter, respectively. The diagonal lines are the lines of identity.

tifies the initial increase in CD11b receptors in patients and is by definition zero for healthy volunteers. t_{CDmax} is the half-life for the return of the CD11b levels in patients to the healthy volunteer levels. MRTCD is the mean residence time for the CD11b and was set to unity as not all of $Rate_{CD}$, MRT_{CD}, and A6(0) (see below) are identifiable simultaneously. θ_{study2} is a correction factor for the higher levels of total CD11b in study 2, resulting from the higher incubation temperature used in the CD11b assay in this study. The fit of the model to the total number of CD11b receptor data is shown in Fig. 4. The initial condition for Eq. (7) was set to $A6(0) = Rate_{CD} \cdot \left(1 + CD_{max} \cdot e^{-\ln 2 \cdot T / t_{CD\,max,i}} + \theta_{study2}\right) \cdot MRT_{CD}$.

PREDICTING THE NUMBER OF FREE CD11b RECEPTORS

The predicted total molar concentration of CD11b receptors $\left(\widehat{CD11b_{N,ij}}\right)$ was obtained by multiplying the predicted number of neutrophils [A4 in Eq. (2)] by the predicted number of CD11b receptors per neutrophil [A6 in Eq. (7)] and dividing by Avogadro's number (N_A):

$$\widehat{CD11b_{N,ij}} = \frac{A6 \cdot A4}{N_A} \tag{8}$$

The predicted number of free CD11b receptors at each time point could then be obtained by the following equation:

$$\widehat{CD11b_{free,ij}} = \widehat{CD11b_{N,ij}}\left(1 - \frac{\widehat{C_{uN,ij}^{\gamma}}}{\widehat{C_{uN,ij}^{\gamma}} + K_D^{\gamma}}\right) \tag{9}$$

where $\widehat{C_{uN,ij}^{\lambda}}$ is the ith individual's jth predicted molar concentration of unbound UK-279,276 (see below) and γ is a modulator that, since it was estimated to be below one, accounts for steric hindrance by already bound UK-279,276

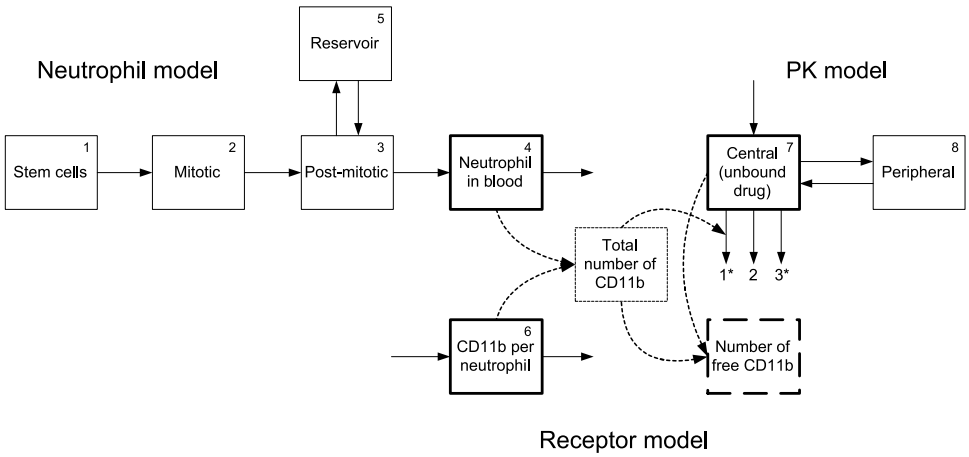

Fig. 6. The full stage 3 model. The dashed arrows indicated dependencies. The thickly lined boxes specify where observations were available: the solidly lined boxes correspond to differential equations while the box with the dashed line indicates a derived quantity.

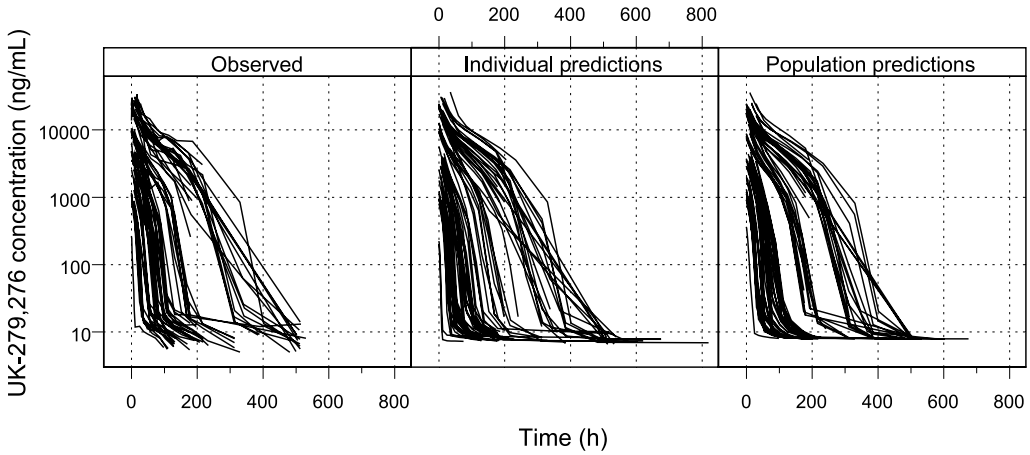

Fig. 7. Observed and predicted (individual and population) UK-279,276 concentrations. Each individual's observations are connected by a line. The graph displays a random selection of about 40% of the total number of individuals.

molecules. The fit of the model to the number of free CD11b receptor data is shown in Fig. 5.

THE MODEL FOR THE PK OF UK-279,276 AND THE SATURABLE BINDING TO THE NEUTROPHILIC CD11b RECEPTORS

The UK-279,276 disposition was found to be adequately described by a two- compartment model with three elimination pathways. The first of these three was a linear (first-order) pathway, the second was nonlinear according to a Michaelis-Menten process, and the third was limited by the total number of free neutrophilic CD11b receptors ($CD11b_{free}$). In terms of differential equations, this model was specified as:

$$\frac{dA7}{dT} = R_0 + \frac{Q_1}{V_2}\cdot A8 - A7\cdot\left(k_{10,ij} + k_{102}\cdot\widehat{CD11b_{free,ij}} + \frac{Q_1}{V_{1,i}}\right) - \frac{V_{max,i}\cdot A7/V_{1,i}}{K_{m,i} + A7/V_{1,i}}$$

$$\frac{dA8}{dT} = \frac{Q_1}{V_{1,i}}\cdot A7 - \frac{Q_1}{V_2}\cdot A8 \qquad (10)$$

where A7 and A8 are the drug amounts in the central and peripheral PK compartments while k_{10} and k_{102} are the rate constants for the linear and CD11b limited pathways, respectively. From a mechanistic standpoint, the linear pathway (k_{10}) is assumed to describe the hepatic desialylation process. Similarly, the Michaelis-Menten pathway is considered to reflect non-neutrophilic CD11b elimination.

FITTING THE MODEL TO THE DATA

The full model is depicted in Fig. 6. In theory it should be possible to fit the whole model to all the observed data simultaneously. This, however, was numerically impossible; thus the full model was split into two parts: the neutrophil model and the receptor+PK model. The two parts of the full model were fitted separately and the receptor+PK part was conditioned on the predictions from the neutrophil part. This approach would give the same results as a simultaneous fitting approach under the assumption that the neutrophil dynamics are independent of drug treatment. The assumption was justified by a graphical inspection of the neutrophil data *vs.* time, stratified by UK-279,276 dose (not shown). In practice this means that A4 in Eq. (8) will be the prediction from the separate fit of the neutrophil part of the full model, to the observed neutrophil counts. The goodness of fit for the PK is shown in Fig. 7 and the parameter estimates are shown in Table III.

Table III. Parameter Estimates from the Final CD11b and PK Model

		Estimate	RSE(%)
$Rate_{CD}$	(1/h)	18700	3.5
$\Theta_{study\ 2}$		0.299	56
CD_{max}		0.259	24
T_{CDmax}	(h)	47.3	27
$V_{max,\ HV}$	(μg/h)	121	5.4
K_m	(μg/L)	48.4	14
V_1	(L)	4.26	2.6
Q_1	(L/h)	96.2	8.0
V_2	(L)	2.73	4.8
K_{10}	(1/h)	3.77	19
K_D	(μg/L)	221	20
γ		373	4.3
K_{102}	(L/(h μg))	0.385	18
WT on $V_{max,HV}$		0.0163	35
$V_{max,p}$	(μg/h)	141	4.9
WT on $V_{max,p}$		0.00862	18
ω_{MRTCD}	(%)	24.5	13
ω_{CDmax}	(%)	172	23
ω_{V1}	(%)	27.7	6.5
ω_{k10}	(%)	84.6	50
ω_{Vmax}	(%)	40.2	13
ω_{KM}	(%)	143	19
ω_{KD}	(%)	90.1	17
$\sigma_{CD,Study\ 2}$	(%)	53.8	7.0
σ_{CD}	(%)	30.2	15
σ_{PK}	(%)	16.8	15
$\sigma_{CD,free}$	(%)	49.5	8.0

COVARIATE ANALYSIS

The volume of distribution for UK-279,276 was estimated to be low, ~7 L (V1+V2, Table III, corresponding to 0.06 L/kg and 0.04 L/kg for V1 and V2, respectively), indicating that its distribution outside plasma is limited owing to its molecular size (48 kDa). Correspondingly, the variability in volume of distribution was estimated to be low ~27% (Table III). Given the modest variability in volume of distribution, no attempt was consequently made to identify any covariate relationships for this parameter. Conversely, the elimination had two components that were expected to vary between individuals in a way that can be explained by covariates. The first is the linear pathway, which is believed to occur in the liver. A correlate of liver size such as weight would be expected to be a predictor for the magnitude of this pathway. The non-neutrophilic pathway accounts for a large proportion of the clearance. If this pathway is related to body size then it is important to attempt to quantify this effect. In addition, it may be different between patients and healthy volunteers as the former probably have up-regulated inflammatory cells as a result of the stroke, and considerably more of the non-neutrophilic CD11b is thought to be situated on cell types that might be expected to be up-regulated following stroke. The variability in the pathway mediated by the neutrophilic CD11b is likely to be explained largely by the predicted total number of binding sites.

When these covariate relationships were tried in the model it was found that V_{max} was indeed higher in patients compared to healthy volunteers. V_{max} was also related to body weight in the expected fashion (increases with increasing body weight). The variability in the linear elimination pathway, on the other hand, could not be explained by body weight.

INTER-INDIVIDUAL AND RESIDUAL VARIABILITY MODELS

In the final model, inter-individual variability could be characterized in kn_1, MSTEP, MRT_{CD}, CD_{max}, V1, k_{10}, V_{max}, K_m, and K_D. Residual variability for all response variables was best described using log-transformed data:

$$\log\left(y_{ij}\right) = \log\left(\hat{y}_{ij}\right) + \varepsilon_{ij} \qquad (11)$$

where y_{ij} is the ith individual's jth observations, $\hat{y}_{ij}$ is the corresponding model prediction, and ε_{ij} is the difference between the two. ε_{ij} is a zero mean, symmetrically distributed variable with standard deviation σ. Four different residual variability terms were estimated, one for each of the PK, the neutrophils, and the free and total number of CD11b receptors per neutrophil.

DISCUSSION

The endpoint of drug development is the approval of a unified drug label that integrates the learning across the various study populations. The implication is that all listed drug attributes can be extrapolated to the population(s) of clinical interest. Commonly, PK/PD findings from healthy volunteers are used to describe many aspects of the general clinical pharmacology (i.e., effect of food, demographic differences, drug–drug interactions, and bioequivalence) and are considered to be directly relevant to the target population. Similarly, the PK/PD from subjects with renal or hepatic impairment and high-dose toleration data from selected subpopulations is considered to apply directly to the wider patient population. The validity of these extrapolations depends on the intrinsic PK/PD properties being the same or establishment of an appropriate bridge to account for any population differences.

The determination of the relationship between the PK measured by the immunoassay and the PD measured by CD11b binding assay was considered key in understanding the clinical pharmacology of UK-279,276. Early in development it was not known whether systemic degradation of UK-279,276 led to a wider distribution of related proteins with differing degrees of affinity to the CD11b receptor, and potential differences in the ability to form complexes with the antibody raised against the parent protein. As a result, the product material detected by the PK assay may not equate to the biologically active protein binding to the CD11b receptor. However, the developed model provides evidence that circulating concentration measured by the PK assay does represent "active" UK-279,276. This finding was important in reducing the need for the logistically difficult CD11b assay in future patient studies.

The lack of concordance between the PK/PD in patients and healthy volunteers was highlighted early in the drug development process and the need to establish a bridge between the populations was considered an important drug development issue. In addition to the rationale discussed earlier, the ability to predict the PD in patients based on healthy volunteer findings was also important in providing a clinical component to the comparability strategy for UK-279,276. Production changes in the system used to produce any protein drug, such as cell bank switches and changes to culture conditions, are inevitable in the scale-up to commercial development. Such changes require that adequate *in vitro* and *in vivo* controls are in place to ensure that the new product is comparable to previous products in terms of efficacy and safety (see CPMP Notes for Guidance on Comparability of Medicinal Products containing Biotechnology-Derived Proteins as Active Substances, www.emea.eu.int, document code EMEA/CPMP/3097/Final). The confidence in the specificity of the PK and binding assays, in addition to the mechanistic understanding of the impact of acute stroke on the PK/PD of UK-279,276, meant that clinical comparability findings in healthy volunteers could be extrapolated to patients.

The successful bridge between healthy volunteers and patients was established by extending the scope and flexibility of the model on the basis of the underlying physiology and pharmacology.

The advantages of taking a mechanistic approach to bridging between healthy volunteers and stroke patients are considered in detail elsewhere (17). However, in brief, the approach provided the opportunity to test and develop hypotheses around the clearance of UK-279,276 and allowed subject matter experts to directly contribute to model development. The mechanistic nature of the model also facil-

itated the propagation of knowledge to the later stages of development, where the sparseness of the data would have otherwise limited interpretation.

From a bridging perspective, the use of empirical models would not have supported the extrapolation to patient populations with different neutrophil counts or CD11b expression. Although patients with signs and symptoms of infection were excluded from this initial patient study (8) these events could significantly alter the neutrophil count. The adoption of the mechanistic approach allows the impact of different neutrophil time courses on the PK/PD to be predicted. In fact, the neutrophil model itself provides the framework for describing how different inflammatory processes would interact with neutrophil proliferation. Further extension of this sub-model may actually allow prediction of changes in the neutrophil count as a function of multiple inflammatory processes.

The mechanistic model highlights that UK-279,276 is an example of a drug that exhibits *target-mediated disposition,* that is, it binds to a receptor or enzyme to the extent that the binding influences the disposition of the drug (18,19). Classical target-mediated drug disposition manifests itself as a (often subtle) dose-dependent decrease in the apparent volume of distribution (18,19). In the case of target-mediated endocytosis, the nonlinear characteristics of the concentration–time profiles become more pronounced (18). According to the present analysis, the PK of UK-279,276 is best described by a model that includes both binding to and elimination from the biological target-the CD11b receptor. In this respect UK-279,276 behaves similarly to the anti-CD11 antibodies HU1124 and Hu23F2G (20,21) and may offer support to the hypothesis that this is a common property of the CD11b receptor. The presence of this hypothesized mechanism allows influence of acute stroke, through CD11b expression, to have a direct dual impact on both the PK and the PD of UK-279,276. In comparison, the use of empirical models would have resulted in disease progression being falsely described as having separate independent effects on the PK and PD components.

Approaches to dealing with covariate modeling for building mechanistic models have, to our knowledge, not been previously discussed. The number of potential parameter–covariate pairs that could be tested increases with increasing complexity. In our case, the partitioning of clearance into separate pathways would have resulted in a lot of covariate testing to strictly define the best fit model by standard stepwise approaches (22,23). When models become complex the ability to undertake standard stepwise approaches is limited by run times. In our case, we limited the extent of the covariate testing by selecting only the covariate–parameter pairs with the strongest mechanistic rationale and the largest scope for providing clinically relevant reductions in unexplained variability.

The role of the PK/PD modeling in the overall development of UK-279,276, including the design and evaluation of the subsequent efficacy trial, is discussed elsewhere (17). Unfortunately, UK-279,276 did not show efficacy in acute ischemic stroke patients (6). However, in preclinical stroke models UK-279,276 showed efficacy only in a transient model of stroke, where reperfusion was established after the initial ischaemia (1,24). Therefore, UK-279,276 may be better as a treatment for reperfusion injury following transient ischemia. Unfortunately, the reperfusion status in patients recruited into the efficacy trial was not known and the best surrogate for reperfusion was concurrent treatment with tissue plasminogen activator (tPA) (which acts by enzymatically lysing the clot). Therefore, the effect of UK-279,276 in preventing reperfusion injury remains unproven. Future applications of UK-279,276, and indeed the family of compounds modulating leukocyte infiltration, may center on other states involving transient ischemia followed by reperfusion, for example, spinal injury, myocardial infarction, and organ transplants. Furthermore, the complex cascade of events following acute stroke may necessitate targeting various stages in the pathogenesis simultaneously (i.e., combination therapy) to produce a clinically significant improvement in outcome in stroke patients. Thus the failure of UK-279,276 as monotherapy in the treatment of the acute stroke population does not itself invalidate CD11b binding as a target for reperfusion injury. Therefore, any future program could benefit from the understanding gained from the mechanistic model developed for UK-279,276.

CONCLUSION

The apparent PK/PD difference between healthy volunteers and patients with acute ischemic stroke treated with UK-279,276 was found to be an artifact of the empirical nature of the initial models tested. A complex mechanistic model that more closely resembled the "true" underlying biology and accounted for an intrinsic disease-dependent target-mediated disposition provided an effective bridge between the populations.

REFERENCES

1. N. Jiang, M. Chopp, and S. Chahwala. Neutrophil inhibitory factor treatment of focal cerebral ischemia in the rat. *Brain Res.* **788**:25–34 (1998).
2. M. Moyle, D. L. Foster, D. E. McGrath, S. M. Brown, Y. Laroche, J. De Meutter, P. Stanssens, C. A. Bogowitz, V. A. Fried, and J. A. Ely *et al.* A hookworm glycoprotein that inhibits neutrophil function is a ligand of the integrin CD11b/CD18. *J. Biol. Chem.* **269**:10008–10015 (1994).
3. R. L. Engler, G. W. Schmid-Schonbein, and R. S. Pavelec. Leukocyte capillary plugging in myocardial ischemia and reperfusion in the dog. *Am. J. Pathol.* **111**:98–111 (1983).
4. M. C. Mazzoni and G. W. Schmid-Schonbein. Mechanisms and consequences of cell activation in the microcirculation. *Cardiovasc. Res.* **32**:709–719 (1996).
5. S. J. Weiss. Tissue destruction by neutrophils. *N. Engl. J. Med.* **320**:365–376 (1989).
6. M. Krams, K. R. Lees, W. Hacke, A. P. Grieve, J. M. Orgogozo, and G. A. Ford. Acute Stroke Therapy by Inhibition of Neutrophils (ASTIN): an adaptive dose-response study of UK-279,276 in acute ischemic stroke. *Stroke* **34**:2543–2548 (2003).
7. M. E. Sughrue and E. S. Connolly Jr. Effectively bridging the preclinical/clinical gap: the results of the ASTIN trial. *Stroke* **35**: e81–e82 (2004). Author reply.
8. K. R. Lees, H. C. Diener, K. Asplund, and M. Krams. UK-279-276, a neutriphil inhibitory glycoprotein, in acute stroke. *Stroke* **34**:1704–1709 (2003).
9. S. L. Beal and L. B. Sheiner. *NONMEM Users Guide, NONMEM Project Group*, University of California, San Francisco, 1998.

10. E. N. Jonsson and M. O. Karlsson. Xpose—an S-PLUS based population pharmacokinetic/pharmacodynamic model building aid for NONMEM. *Comput. Methods Programs Biomed.* **58**:51–64 (1999).
11. U. Wahlby, E. N. Jonsson, and M. O. Karlsson. Assessment of actual significance levels for covariate effects in NONMEM. *J. Pharmacokinet. Pharmacodyn.* **28**:231–252 (2001).
12. U. Wahlby, M. R. Bouw, E. N. Jonsson, and M. O. Karlsson. Assessment of type I error rates for the statistical sub-model in NONMEM. *J. Pharmacokinet. Pharmacodyn.* **29**:251–269 (2002).
13. H. Kato, K. Kogure, X. H. Liu, T. Araki, and Y. Itoyama. Progressive expression of immunomolecules on activated microglia and invading leukocytes following focal cerebral ischemia in the rat. *Brain Res.* **734**:203–212 (1996).
14. R. Webster, J. Phipps, R. Hyland, and D. Walker. Evaluation of the role of the asialoglycoprotein receptor in the clearance of UK-279,276 (recombinant neutrophil inhibitory factor). *Xenobiotica* **33**:945–956 (2003).
15. L. E. Friberg, A. Henningsson, H. Maas, L. Nguyen, and M. O. Karlsson. Model of chemotherapy-induced myelosuppression with parameter consistency across drugs. *J. Clin. Oncol.* **20**:4713–4721 (2002).
16. R. I. Walker and R. Willemze. Neutrophil kinetics and the regulation of granulopoiesis. *Rev. Infect. Dis.* **2**:282–292 (1980).
17. S. Marshall, F. Macintyre, I. James, M. Krams, and E. N. Jonsson. Application of a mechanistically based pharmacokinetic/pharmacodynamic model in the development of neutrophil inhibitory factor UK-279,276 for the treatment of ischaemic stroke. *Accepted for publication in Clin Pharmacokinet* (2005).
18. D. E. Mager and W. J. Jusko. General pharmacokinetic model for drugs exhibiting target-mediated drug disposition. *J. Pharmacokinet. Pharmacodyn.* **28**:507–532 (2001).
19. G. Levy. Pharmacologic target-mediated drug disposition. *Clin. Pharmacol. Ther.* **56**:248–252 (1994).
20. J. D. Bowen, S .H. Petersdorf, T. L. Richards, K. R. Maravilla, D. C. Dale, T. H. Price, T. P. St John, and A. S. Yu. Phase I study of a humanized anti-CD11/CD18 monoclonal antibody in multiple sclerosis. *Clin. Pharmacol. Ther.* **64**:339–346 (1998).
21. R. J. Bauer, R. L. Dedrick, M. L. White, M. J. Murray, and M. R. Garovoy. Population pharmacokinetics and pharmacodynamics of the anti-CD11a antibody hu1124 in human subjects with psoriasis. *J. Pharmacokinet. Biopharm.* **27**:397–420 (1999).
22. E. N. Jonsson and M. O. Karlsson. Automated covariate model building within NONMEM. *Pharm. Res.* **15**:1463–1468 (1998).
23. J. W. Mandema, D. Verotta, and L. B. Sheiner. Building population pharmacokinetic-pharmacodynamic models. I. Models for covariate effects. *J. Pharmacokinet. Biopharm.* **20**:511–528 (1992).
24. L. Zhang, Z. G. Zhang, R. L. Zhang, M. Lu, M. Krams, and M. Chopp. Effects of a selective CD11b/CD18 antagonist and recombinant human tissue plasminogen activator treatment alone and in combination in a rat embolic model of stroke. *Stroke* **34**:1790–1795 (2003).